2023 45th Annual International Conference of the IEEE Engineering in Medicine & Biology Society (EMBC) | 979-8-3503-2447-1/23/$31.00 ©2023 IEEE | DOI: 10.1109/EMBC40787.2023.10340629

Characterization of the Optical and Thermal Properties of Cardiac Tissue as a Function of Temperature

Leonardo Bianchi, *Graduate Student Member, IEEE*, Alessandro Bossi, Antonio Pifferi, and Paola Saccomandi, *Senior Member, IEEE*

***Abstract*— In this work, we devised the first characterization of the optical and thermal properties of *ex vivo* cardiac tissue as a function of different selected temperatures, ranging from room temperature to hyperthermic and ablative temperatures. The broadband (i.e., from 650 nm to 1100 nm) estimation of the optical properties, i.e., absorption coefficient (μ_a) and reduced scattering coefficient (μ'_s), was performed by means of time-domain diffuse optics. Besides, the measurement of the thermal properties was based on the transient hot-wire technique, employing a dual-needle probe to estimate the tissue thermal conductivity (k), thermal diffusivity (α), and volumetric heat capacity (C_v). Increasing the tissue temperature led to variations in the spectral characteristics of μ_a (e.g., the redshift of the 780 nm peak, the rise of a new peak at 840 nm, and the formation of a valley at 900 nm). Moreover, an increase in the values of μ'_s was assessed as tissue temperature raised (e.g., for 800 nm, at 25 °C μ'_s= 9.8 cm^{-1}, while at 77 °C μ'_s= 29.1 cm^{-1}). Concerning the thermal properties characterization, k was almost constant in the selected temperature interval. Conversely, α and C_v were subjected to an increase and a decrease with temperature, respectively; thus, they registered values of 0.190 mm^2/s and 3.03 MJ/(m^3·K) at the maximum investigated temperature (79 °C), accordingly.**

***Clinical Relevance*— The experimentally obtained optical and thermal properties of cardiac tissue are useful to improve the accuracy of simulation-based tools for thermal therapy planning. Furthermore, the measured properties can serve as a reference for the realization of tissue-mimicking phantoms for medical training and testing of medical instruments.**

I. Introduction

Accurate information on the physical properties of biological tissues is fundamental for improving diagnostic and therapeutic procedures and medical treatments. Hence, many efforts have been devoted, in the field of bioengineering, to the evaluation of optical, thermal, mechanical, and dielectric properties of biological media [1], [2]. In this regard, the investigation of the optical and thermal behavior of tissues is pivotal for the realization of tissue-mimicking materials [3], [4], employed for fine-tuning and the pre-clinical testing of medical devices, as well as for medical training, and the implementation of numerical models for therapy preplanning. These models are indeed useful to foresee the outcome of interventional procedures and select the best treatment strategy [5]–[7]. However, their accuracy and prediction capabilities are strictly related to given input physical parameters, such as the optical and thermal properties of tissue [2], [8].

The tissue optical properties, such as absorption (μ_a) and scattering (μ_s) coefficients, regulate the light propagation within the biological material. While μ_a is a measure of how far light can travel through the biological material prior to being absorbed, the direction of light propagation is determined by μ_s. Moreover, considering the tissue anisotropy factor g, the reduced scattering coefficient (μ'_s) can be defined: $\mu'_s = \mu_s (1 - g)$. Tissue optical properties depend on the wavelength of the light interacting with the tissue itself, thus they should be investigated in a broad wavelength range for the thorough identification of the tissue spectral features [8]–[10].

The heat distribution in biological tissues is instead affected by the so-called tissue thermal properties. The thermal conductivity (k) quantifies the heat conduction capability of tissues, the volumetric heat capacity (C_v) is defined as the product between the tissue specific heat c and the tissue density ρ ($C_v = \rho c$), whilst the thermal diffusivity α is expressed as the ratio between k and C_v ($\alpha = k/C_v$) and it defines the ability of the tissue to transfer thermal energy in proportion to its ability to store heat [2], [11]–[13].

Technological advancements in the biomedical field have led to the possibility of quantitatively assessing the optical and thermal response of biological tissues of interest, such as cardiac tissue. Indeed, the exploration of the optical properties of the heart may be beneficial for the refinement of therapeutic applications in laser medicine, e.g., low-level laser therapy after myocardial infarction [14], and other biophotonic applications involving this organ. Furthermore, detailed knowledge of the thermal properties of cardiac tissue can help increase the effectiveness of thermal treatments and heart ablation procedures, for the treatment of arrhythmias or atrial fibrillation [15], [16].

Despite the need for detailed information on the physical properties of the heart, the studies available in the literature on the optical and thermal properties of cardiac tissue are still limited and typically investigated these properties at baseline conditions without considering their possible variation according to tissue temperature [2], [17]. In this regard, to further enlighten the temperature dependence of the optical

*This project has received funding from the European Research Council (ERC) under the European Union's Horizon 2020 research and innovation programme (Grant agreement No. 759159). This work was also funded by Fondazione Cariplo (grant n° 2017-2075).

Leonardo Bianchi is with the Department of Mechanical Engineering, Politecnico di Milano, 20156 Milan, Italy (corresponding author to provide e-mail: leonardo.bianchi@polimi.it).

Alessandro Bossi and Paola Saccomandi are with the Department of Mechanical Engineering, Politecnico di Milano, 20156 Milan, Italy (e-mail: alessandro.bossi@polimi.it, paola.saccomandi@polimi.it).

Antonio Pifferi is with the Department of Physics, Politecnico di Milano, Milan, 20133, Italy, and the Institute of Photonics and Nanotechnologies, National Research Council, Milan, 20133, Italy (e-mail: antonio.pifferi@polimi.it).

and thermal properties of the heart tissue, our work presents the first broad wavelength (i.e., from 650 nm to 1100 nm) characterization of optical properties as well as the estimation of the thermal properties of cardiac tissue as a function of different physiological and supraphysiological temperatures.

II. Materials and Methods

A. Preparation of tissue samples

The measurements of the optical and thermal properties were performed on *ex vivo* heart tissues (atrial tissue and ventricles) excised from healthy animals and obtained from a local butchery. Valves and blood clots were accurately removed prior to positioning the tissue samples in a metallic container. Hence, the filled container was sealed and moved inside a water thermal bath (IVYX Scientific Laboratory Digital Water Bath). The thermal bath was then utilized to bring the sample to several selected temperatures at which the optical and thermal properties were measured. The tissue temperatures as well as the water temperature were assessed by means of k-type thermocouples (0.1 °C accuracy) connected to a temperature monitoring module (Yokogawa FX1000 Paperless Recorder).

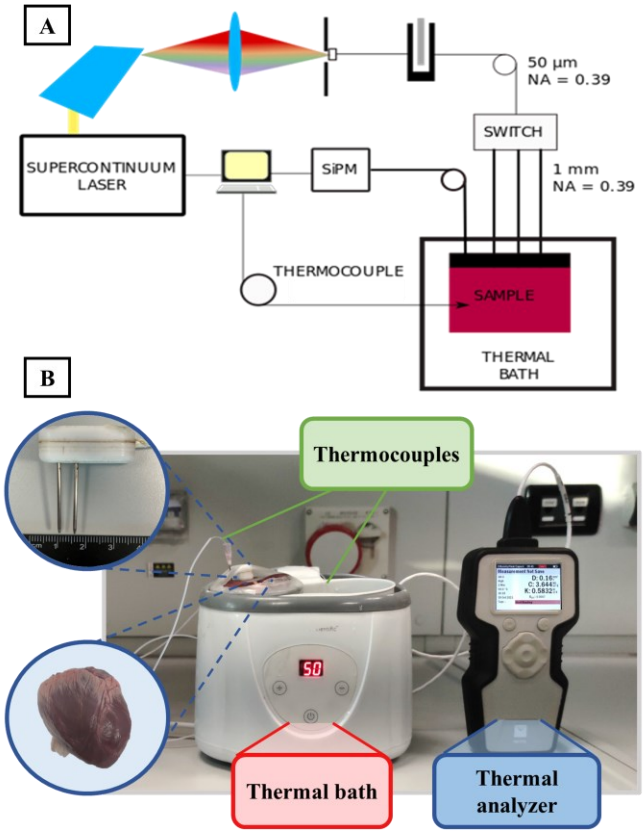

Figure 1. (A) Experimental setup utilized for the estimation of the optical properties of cardiac tissue. (B) Experimental setup used for the measurement of the thermal properties of heart tissue.

B. Measurement of the optical properties

To measure μ_a and μ'_s in relation to temperature, bovine heart tissue samples were uniformly heated for 4 hours using the thermal bath which kept the tissue temperature approximately constant at a set temperature (25 °C, 37 °C, 59 °C, and 77 °C). The optical properties were measured using time-domain diffuse optics. The setup scheme is presented in Fig. 1. We selected a single wavelength using a prism from a supercontinuum laser [8] and sent it into the sample. We collected the diffused light at 1 cm from the injection point in reflectance configuration and integrated each curve for 1 s. We used a silicon photomultiplier (SiPM) to measure the time of arrival of photons and we used time-correlated single photon counting to reconstruct the distributed time of flight (DTOF). The spectra of the optical properties were retrieved by fitting the measured DTOF to a solution of the diffuse equation. The spectra were measured every 10 nm from 650 nm to 1100 nm. The temporal point spread function has 60 ps of full width at half maximum. The measurements of the optical properties were repeated three times at each temperature.

C. Measurement of the thermal properties

Once the selected tissue temperature and the thermal equilibrium within the sample were achieved, k, C_v, and α were estimated by means of the transient hot-wire technique, using porcine heart tissues. A dual-needle probe (TEMPOS SH-3) consisting of two needles (30 mm in length, located at a distance r of 6 mm from each other and with a diameter of 1.3 mm) was employed. The probe allowed to record the initial temperature of the tissue by the monitoring needle, deliver a specific amount of heat q to the specimen by means of the heating needle for a time equal to 30 s (t_h), and measure the resulting localized tissue temperature variation ΔT (typically <1 °C compared to the initial temperature) for the following 90 s. The probe was connected to a thermal property analyzer (TEMPOS, Meter Group, Inc., Pullman, WA, USA, 10% accuracy; an instrument in accordance with ASTM 5334 and IEEE 442).

The thermal properties were then estimated by the analyzer, which computes the minimization of mean square error between the measured temperature changes and those obtained by a mathematical heat transfer model, implemented in the software of the system. In particular, the k and α are estimated by the thermal analyzer through the following equations [11], [18]:

$$\Delta T = \left[\frac{q}{4\pi k}\right] E_i\left[\frac{-r^2}{4\alpha t}\right] \qquad t \le t_h \qquad (1)$$

$$\Delta T = \left[\frac{q}{\pi k}\right]\left\{E_i\left[\frac{-r^2}{4\alpha(t-t_h)}\right] - E_i\left[\frac{-r^2}{4\alpha t}\right]\right\} \qquad t > t_h \qquad (2)$$

in which E_i is the exponential integral [19] and t is the time. Moreover, through the formula $C_v = k/\alpha$, it is possible to attain the value of C_v [11]. The measurements were performed in triplicates at each temperature value.

III. Results and Discussion

A. Optical properties of cardiac tissue

In Fig. 2.A, the values of μ_a as a function of wavelength, λ, for the selected tissue temperatures are shown. A tiny decrease in the intensity between the native state (i.e., 25 °C) and 37 °C and a higher reduction from 37 °C to 59 °C can be observed. They are likely linked with inaccuracies in the diffusion

model. At 77 °C, significant changes in the spectral features appear. Firstly, a redshift of the 780 nm peak due to changes in the mode of vibration of deoxy-myoglobin [20] can be noticed (green circle). Then, at 840 nm the rise of a new peak linked with met-myoglobin formation (gray circle) [20] and the formation of a valley at 900 nm (light blue circle) are observable. The decrease of μ_a in the region 800-900 nm after 70 °C is also due to tissue water evaporation [21], [22]. In Fig. 3.A, we present the values of μ_a at 800 nm, at the different temperatures. Again, we can observe the decline in μ_a up to 59 °C and then an increase likely linked with the formation of met-myoglobin.

Fig. 2.B shows the spectra of μ'_s. The spectra features are mainly linked with the microstructural characterization, in particular, the protein state. A slight increase in μ'_s can be observed from the native state to the tissue treated at 37 °C. From 37 °C to 59 °C, we observe a significant increase in the values of μ'_s and a smaller increase from 59 °C to 77 °C. The increase in μ'_s is mainly likely linked with myosin denaturation [23]. In Fig. 3.B, we can see a constant increase in μ'_s at 800 nm with temperature, ascribable to the increasing denaturation of the proteins at higher temperatures.

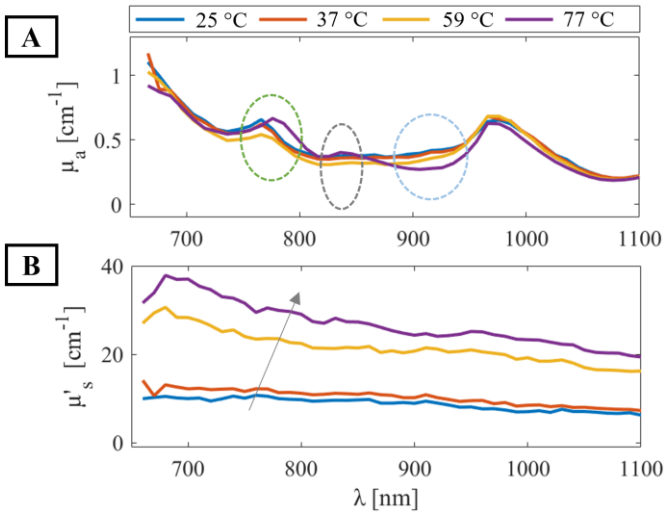

Figure 2. (A) Spectra of the absorption coefficient μ_a and (B) spectra of the reduced scattering coefficient μ'_s for cardiac tissue as a function of wavelength λ (from 650 nm to 1100 nm) at different cardiac tissue temperatures.

B. *Thermal properties of cardiac tissue*

The thermal properties of *ex vivo* cardiac tissue, as a function of the different selected temperatures, are reported in

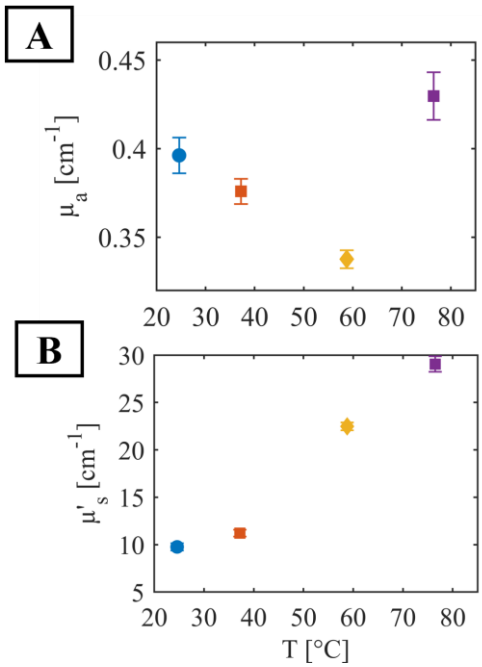

Figure 3. (A) Absorption coefficient μ_a and (B) reduced scattering coefficient μ'_s for cardiac tissue as a function of different selected temperatures at the wavelength λ of 800 nm. The error bars represent the standard deviation of the mean.

Fig. 4. The k remained approximately constant in the investigated temperature range (Fig. 4.A), showing minimum and maximum average values equal to 0.560 W/(m·K) and 0.585 W/(m·K), respectively. Differently from the behavior of k, the tissue α appeared rather constant up to 55 °C, then, at a temperature close to 79 °C, it experienced a 1.2-fold increase compared to its nominal value (Fig. 4.B). The maximum value reached at ~79 °C was equal to 0.190 mm^2/s. The C_v was not subjected to substantial changes up to 55 °C. Afterward, it subsided with increasing temperature, showing a value of 3.03 MJ/(m^3·K) at 79 °C. The low values of the standard deviation of the mean (Fig. 4) associated with the three measurement repetitions, performed at each temperature, denoted good intra-sample measurement repeatability.

Overall, the average values of thermal properties and their trend as a function of temperature are in line with the measurement performed on other biological tissues with the transient hot-wire technique and the dual-needle probe [17], [24]. Moreover, the present results are in agreement with

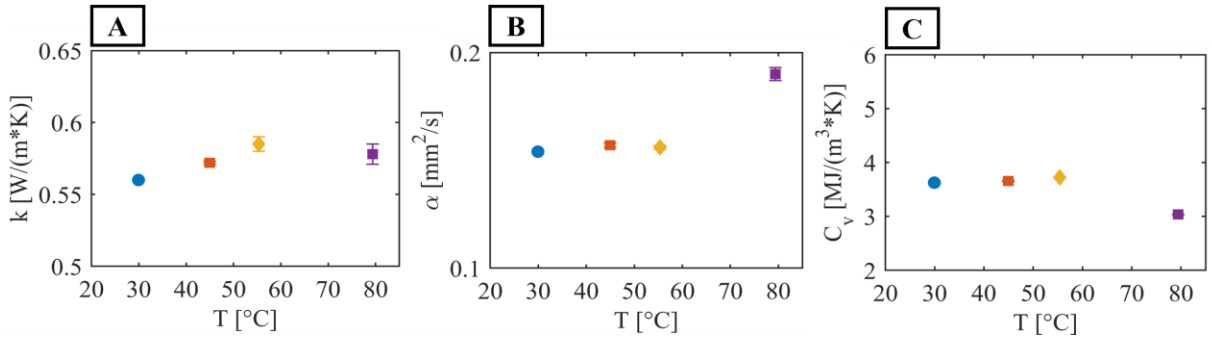

Figure 4. Thermal properties of cardiac tissue as a function of different selected temperatures: (A) tissue thermal conductivity k, (B) thermal diffusivity α, and (C) volumetric heat capacity C_v. The error bars represent the standard deviation of the mean.

previous investigations in *ex vivo* porcine myocardial tissue, in which the thermal properties were measured with a self-heated-thermistor probe [25]. The variation in the thermal properties at higher tissue temperatures may be explicable by changes in the tissue water content. Indeed, it has been shown in the literature that at higher temperatures and, in particular, approaching the onset of water vaporization, thermal properties can undergo substantial variations compared to their nominal values at room temperature [2], [17], [24], [26].

IV. Conclusion

This work proposes the estimation of the optical and thermal properties of *ex vivo* cardiac tissues as a function of different selected temperatures, from room to ablative temperatures. Time-domain diffuse optics was used to estimate μ_a and μ'_s as a function of wavelength (from 650 nm to 1100 nm) at different temperatures. The transient hot-wire technique was employed to estimate the tissue thermal properties, i.e., k, α, and C_v. The increase of tissue temperature induced variations in the spectral features of μ_a. Besides, an increment in μ'_s with temperature was assessed. Regarding the thermal properties of cardiac tissue, an increase in α and a decrease in C_v were registered at the maximum investigated value, i.e., 79 °C. In conclusion, the presented optical and thermal properties are useful for the implementation of more accurate computational frameworks for therapy preplanning and for the realization of phantoms mimicking tissue behavior. Further studies should focus on the characterization of the physical properties of human healthy and diseased tissues, as well as on their investigation in physiological-like conditions resembling the *in vivo* scenario.

References

[1] C. Rossmann and D. Haemmerich, "Review of Temperature Dependence of Thermal Properties, Dielectric Properties, and Perfusion of Biological Tissues at Hyperthermic and Ablation Temperatures," *Crit Rev Biomed Eng*, vol. 42, no. 6, pp. 467–492, 2014, doi: 10.1615/CritRevBiomedEng.2015012486.

[2] L. Bianchi, F. Cavarzan, L. Ciampitti, M. Cremonesi, F. Grilli, and P. Saccomandi, "Thermophysical and mechanical properties of biological tissues as a function of temperature: a systematic literature review," *International Journal of Hyperthermia*, vol. 39, no. 1, pp. 297–340, Dec. 2022, doi: 10.1080/02656736.2022.2028908.

[3] J. R. Cook, R. R. Bouchard, and S. Y. Emelianov, "Tissue-mimicking phantoms for photoacoustic and ultrasonic imaging," *Biomed Opt Express*, vol. 2, no. 11, p. 3193, Nov. 2011, doi: 10.1364/BOE.2.003193.

[4] L. Bianchi, S. Asadi, M. de Landro, S. Korganbayev, and P. Saccomandi, "Measurement of thermal properties of biological tissues and tissue-mimicking phantom with a dual-needle sensor," in *2022 IEEE International Symposium on Medical Measurements and Applications (MeMeA)*, Nov. 2022, pp. 1–6. doi: 10.1109/MeMeA54994.2022.9856408.

[5] A. Mohammadi, L. Bianchi, S. Korganbayev, M. de Landro, and P. Saccomandi, "Thermomechanical Modeling of Laser Ablation Therapy of Tumors: Sensitivity Analysis and Optimization of Influential Variables," *IEEE Trans Biomed Eng*, 2021, doi: 10.1109/TBME.2021.3092889.

[6] S. J. Payne, T. Peng, and D. P. O'Neill, "Mathematical modeling of thermal ablation," *Critical Reviews in Biomedical Engineering*. 2010.

[7] L. Bianchi, S. Korganbayev, A. Orrico, M. de Landro, and P. Saccomandi, "Quasi-distributed fiber optic sensor-based control system for interstitial laser ablation of tissue: theoretical and experimental investigations," *Biomed. Opt. Express*, vol. 12, no. 5, pp. 2841–2858, May 2021, doi: 10.1364/BOE.419541.

[8] P. Lanka, L. Bianchi, A. Farina, M. de Landro, A. Pifferi, and P. Saccomandi, "Estimation of porcine pancreas optical properties in the 600–1100 nm wavelength range for light-based therapies," *Sci Rep*, vol. 12, no. 1, p. 14300, Aug. 2022, doi: 10.1038/s41598-022-18277-7.

[9] S. Mosca *et al.*, "Optical characterization of porcine tissues from various organs in the 650–1100 nm range using time-domain diffuse spectroscopy," *Biomed Opt Express*, vol. 11, no. 3, p. 1697, Nov. 2020, doi: 10.1364/BOE.386349.

[10] S. Akter *et al.*, "Evaluation of light scattering and absorption properties of in vivo rat liver using a single-reflectance fiber probe during preischemia, ischemia–reperfusion, and postmortem," *J Biomed Opt*, vol. 20, no. 7, p. 76010, Nov. 2015, doi: 10.1117/1.JBO.20.7.076010.

[11] A. Mohammadi, L. Bianchi, S. Asadi, and P. Saccomandi, "Measurement of Ex Vivo Liver, Brain and Pancreas Thermal Properties as Function of Temperature," *Sensors*, vol. 21, no. 12, p. 4236, Jun. 2021, doi: 10.3390/s21124236.

[12] P. Nesvadba, "A new transient method of the measurement of temperature dependent thermal diffusivity," *J Phys D Appl Phys*, vol. 15, no. 5, pp. 725–738, May 1982, doi: 10.1088/0022-3727/15/5/003.

[13] W. Buck and S. Rudtsch, "Thermal Properties," in *Springer Handbook of Materials Measurement Methods*, H. Czichos, T. Saito, and L. Smith, Eds. Berlin, Heidelberg: Springer Berlin Heidelberg, 2006, pp. 399–429. doi: 10.1007/978-3-540-30300-8_8.

[14] U. Oron *et al.*, "Low-Energy Laser Irradiation Reduces Formation of Scar Tissue After Myocardial Infarction in Rats and Dogs," *Circulation*, vol. 103, no. 2, pp. 296–301, Jan. 2001, doi: 10.1161/01.CIR.103.2.296.

[15] F. W. Mohr *et al.*, "Curative treatment of atrial fibrillation with intraoperative radiofrequency ablation: Short-term and midterm results," *J Thorac Cardiovasc Surg*, vol. 123, no. 5, pp. 919–927, 2002, doi: https://doi.org/10.1067/mtc.2002.120730.

[16] M. la Meir *et al.*, "Minimal invasive surgery for atrial fibrillation: an updated review," *EP Europace*, vol. 15, no. 2, pp. 170–182, Nov. 2013, doi: 10.1093/europace/eus216.

[17] A. Mohammadi, L. Bianchi, S. Asadi, and P. Saccomandi, "Measurement of Ex Vivo Liver, Brain and Pancreas Thermal Properties as Function of Temperature," *Sensors*, vol. 21, no. 12, p. 4236, Jun. 2021, doi: 10.3390/s21124236.

[18] N. P. Silva, A. Bottiglieri, R. C. Conceição, M. O'Halloran, and L. Farina, "Characterisation of Ex Vivo Liver Thermal Properties for Electromagnetic-Based Hyperthermic Therapies," *Sensors*, vol. 20, no. 10, p. 3004, May 2020, doi: 10.3390/s20103004.

[19] M. Abramowitz, I. A. Stegun, and R. H. Romer, "Handbook of Mathematical Functions with Formulas, Graphs, and Mathematical Tables," *Am J Phys*, vol. 56, no. 10, p. 958, Oct. 1988.

[20] P. Lanka *et al.*, "Time domain diffuse optical spectroscopy for the monitoring of thermal treatment in biological tissue.," in *Biophotonics Congress: Biomedical Optics 2020 (Translational, Microscopy, OCT, OTS, BRAIN)*, 2020, p. SM2D.4. doi: 10.1364/OTS.2020.SM2D.4.

[21] M. de Landro *et al.*, "Prediction of In Vivo Laser-Induced Thermal Damage with Hyperspectral Imaging Using Deep Learning," *Sensors*, vol. 21, no. 20, 2021, doi: 10.3390/s21206934.

[22] M. de Landro *et al.*, "Hyperspectral Imagery for Assessing Laser-Induced Thermal State Change in Liver," *Sensors*, vol. 21, no. 2, 2021, doi: 10.3390/s21020643.

[23] H. C. Bertram, Z. Wu, F. van den Berg, and H. J. Andersen, "NMR relaxometry and differential scanning calorimetry during meat cooking," *Meat Sci*, vol. 74, no. 4, pp. 684–689, 2006, doi: https://doi.org/10.1016/j.meatsci.2006.05.020.

[24] N. P. Silva, A. Bottiglieri, R. C. Conceição, M. O'Halloran, and L. Farina, "Characterisation of Ex Vivo Liver Thermal Properties for Electromagnetic-Based Hyperthermic Therapies," *Sensors*, vol. 20, no. 10, 2020, doi: 10.3390/s20103004.

[25] N. C. Bhavaraju and J. W. Valvano, "Thermophysical Properties of Swine Myocardium," *Int J Thermophys*, vol. 20, no. 2, pp. 665–676, 1999, doi: 10.1023/A:1022673524963.

[26] L. Bianchi, M. Bontempi, S. de Simone, M. Franceschet, and P. Saccomandi, "Temperature Dependence of Thermal Properties of Ex Vivo Porcine Heart and Lung in Hyperthermia and Ablative Temperature Ranges," *Ann Biomed Eng*, 2023, doi: 10.1007/s10439-022-03122-9.